

15th CIRP Conference on Modelling of Machining Operations

Considering the Influence of Minimum Quantity Lubrication for Modelling Changes in Temperature, Forces and Phase Transformations during Machining

Patrick Bollig^{a*}, Carsten Faltin^b, Robert Schießl^b, Johannes Schneider^c, Ulrich Maas^b,
Volker Schulze^a

^awbk Institute of Production Science, Kaiserstraße 12, Karlsruhe 76131, Germany

^bITT Institute of Technical Thermodynamics, Kaiserstraße 12, Karlsruhe 76131, Germany

^cIAM-ZBS Institute of Applied Materials Reliability of Components and Systems, Kaiserstraße 12, Karlsruhe 76131, Germany

* Corresponding author. Tel.: +49-721-608-47865; fax: +49-721-608-45005. E-mail address: Patrick.Bollig@kit.edu

Abstract

The purpose of this study aims at presenting a method for modelling machining processes considering Minimum Quantity Lubrication (MQL) in a 2D and 3D FEM simulation by using the example of machining tempered steel AISI 4140. All parameters required for the FEM simulation are calculated within the multiphase simulation code INSFLA and the formula for the heat conduction coefficient is derived. To consider the influence of phase transformations of the fluid, separate experiments are performed. Furthermore, the friction coefficient is measured experimentally in dependence of the relative sliding velocity, contact pressure and temperature during machining with MQL as well as under dry conditions. The extended friction model is used for the 2D and 3D models. MQL machining experiments are performed for the purpose of validating these models. The main focus of the experiments is laid on cutting temperatures, forces and phase transformations on single workpieces.

© 2015 The Authors. Published by Elsevier B.V. This is an open access article under the CC BY-NC-ND license

(<http://creativecommons.org/licenses/by-nc-nd/4.0/>).

Peer-review under responsibility of the International Scientific Committee of the “15th Conference on Modelling of Machining Operations

Keywords: Finite element method (FEM), machining, simulation, lubrication, cooling

1. INTRODUCTION

Minimum Quantity Lubrication (MQL) is a widely used machining technology in industry and research. The main machining processes, the MQL is applied to, are drilling [1], turning [2] or milling [3]. As a mixture of wet and dry machining, the MQL technique combines the positive effects of both methods. The benefits of MQL are evident in many areas such as minimizing manufacturing costs, legal demands or human health [4]. The influence of the process parameters like cutting speed, depth of cut, feed or nozzle position on temperature, surface roughness and machining forces in turning have been examined by Hadad et al. [5]. It has been shown that the machining forces and temperatures are lower than in dry machining or flooded cooling. This causes a better tool chip interaction because of lower wear and better surface roughness. The nozzle position affects the supplied oil mist and the coating applied to the rake face and flank face. [6]

combined MQL with supercritical CO₂ during external turning. Lower tool wear and higher material removal rate compared to aqueous flood coolant was shown.

However, MQL has rarely been investigated in the modelling of machining operations. This is mainly due to the enhanced amount of computer performance and time to simulate the heat transfers between the workpiece/tool and the fluid. Furthermore, there is a lack of knowledge on how the effects of MQL can be explained and considered [7].

When a cooling fluid is modelled in a simulation, a computational fluid dynamics (CFD) approach is typically used. With this kind of simulation, the flow of the fluid between a nozzle and the workpiece/tool is usually examined [8, 9]. These investigations are often performed without considering the heat transfer between the fluid and the machining process [10, 11] which makes it impossible to calculate the influence of the cooling and lubrication effects on the maximum temperature [8]. A detailed examination, for

example, of the phase transformation in the surface layer cannot be done without considering the maximum temperature. Another problem of CFD simulation arises in the fact that the mechanical properties of solid components and therefore chip formation cannot be simulated. For this reason, [8, 9, 10, 11] disregard the chip formation and only use a moving heat source even when a machining operation is simulated with a defined cutting edge.

In the work of Pervaiz et al., a separated modelling approach is presented [12]. First of all, a 2D orthogonal cutting FEM model calculates the temperature distribution during the cutting process. After this simulation, the thermal results are used in a CFD simulation of the cutting tool to compare the influence of dry machining to a flooded cooling. The calculated results show encouraging concordance. A similar modelling approach can be found in [13].

In this paper, a 2D chip formation and 3D drilling finite element simulation considering MQL shall be presented. In addition to the work of [14], the tool forms part of the simulation.

2. General approach

The following sections will introduce the modelling approach for the machining simulations with MQL and the experimental investigations. A deeper look into the modelling parts of thermal and mathematical description of the MQL and the thermal dependence to the frictional behaviour while machining with MQL.

2.1. Friction modelling

The frictional behaviour of the tribo couple cutting tool/workpiece is characterized as a function of sliding speed, temperature and lubricant at load conditions (contact pressure, sliding speed, media) covering the complete range of the machining parameters used for the drilling of the workpieces (see section 2.5) Therefore, a laboratory tribometer of type CETR UMT3 is used for performing load cycle tests with triangular cutting tools (width 4.8 mm; contact radius 0.4 mm) made of uncoated and PVD coated (TiCN) cemented carbide in contact with tempered AISI 4140 steel discs at a normal load of 20 N. During the tests at room temperature and 50% rh, the sliding speed is increased from 0 to 10 m/sec within 5 sec, held for 5 sec and then decreased again to 0 m/sec a 100 times and the temperature of the cutting tool is continuously measured by a thermocouple about half a millimetre below the tribological contact. Tests are run unlubricated (with and without additional cooling air flow) as well as lubricated with cutting fluid (MAG CYCLO COOL 20 MU, 5% concentration in distilled water), pure distilled water and hexadecane (model fluids for the heat transfer simulations). The data shown in the following figures are all obtained from the 21st to the 100th load cycle to eliminate the influence of running in effects.

Figure 1 exemplarily presents the friction coefficient as a function of sliding speed and temperature for the unlubricated sliding couple with uncoated cutting tool. It can be seen that the level of the friction coefficients and temperatures is

significantly lower than in dry conditions. In addition, Table 1 shows the average values of these experiments

Table 1: Results of the tribological experiments

cutting tool	test conditions	T average °C	μ average
uncoated	dry, 50% rh	250	0.58
	dry, 50% rh + airflow	195	0.54
	cutting fluid	34	0.08
	distilled water	30	0.08
Coated	hexadecane	44	0.06
	dry, 50% rh	161	0.55

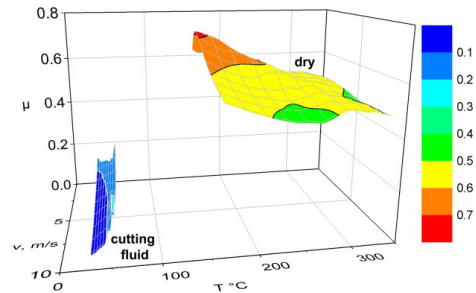


Figure 1: Friction coefficients as function of sliding speed and temperature for the uncoated cutting tool versus tempered AISI 4140 steel during tribological model test ($F_N = 20$ N, $v = 0 - 10$ m/s, 50% rh, unlubricated and lubricated with cutting fluid, data obtained from load ramps 21 to 100 to eliminate running in effects)

Figure 2 summarises the results of the tribological model tests under the different test conditions. It is obvious that, for all sliding pairs, the friction coefficient decreases with increasing sliding speed as well as with increasing temperature. Under dry conditions, the PVD coating of the cutting tool results in a reduced friction coefficient for sliding speeds above 3 m/sec and a lower temperature. Under lubricated test conditions, both, the friction coefficient and the temperature, show a reduced sliding speed dependence and a significantly lower level of the two parameters compared to the unlubricated tests. Under lubricated conditions the PVD coated cutting tools do not show significantly different results compared to the uncoated cutting tools.

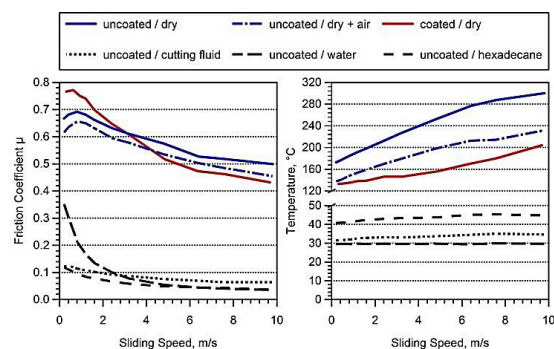


Figure 2: Comparison of the friction coefficient and the temperature during tribological model test with under different test conditions

The results of the tribological model tests are implemented in the FE machining model as a function of the friction coefficients in dependence of sliding speed and temperature.

2.2. Mathematical description of the MQL

In conventional FEM simulations, the convective heat transfer from solid to cooling fluid (and vice versa) is regularly neglected due to the large computational effort associated with this effect. A detailed simulation of this heat transfer rate requires knowledge of several material parameters (e.g. heat conductivities, heat capacities, viscosities) which usually exhibit a complex state dependence. Furthermore, it calls for detailed information of the temperature gradient of fluid and solid at the fluid/wall interface. In order to realistically compute this transfer, the spatial temperature field has to be fully resolved in the cutting simulation. This detailed modelling causes a large computational effort in the numerical solution and makes it a non-standard technique for engineering scale.

The following three-step strategy has been used as an approach to master the just mentioned problems and to allow realistic heat transfer modelling, also in FEM simulations of practical systems:

1. Fully detailed and fully resolved numerical simulations of the fluid-wall heat transfer process for simple, generic geometries (boundary layer flow). These simulations are parameterised by the fluid mass flux, fluid core temperature, wall surface temperature. Additionally, the solid-fluid heat transfer is observed to be dependent on the contact duration of fluid and wall. These simulations are performed by the in-house code INSFLA [15] for simulations of reacting flows in simple geometries. The simulations include state-dependent thermodynamical fluid properties (like heat capacity, viscosity and thermal conductivity), as well as full resolution of the fluid-wall boundary layer.
2. Extraction of parameter- and time dependent effective heat transfer coefficients from the detailed, simple generic scenarios as a function of the selected parameters, and tabulation of this multi-dimensional function for later use in FEM simulations.
3. Use of the tabulated heat transfer rate coefficients in FEM simulations of machining processes as additional terms for computing the temperature field in fluids and solids. The FEM code supplies local wall temperatures, the initial fluid temperature, fluid flow rate, and the contact time between wall and fluid to obtain the heat transfer coefficients from the pre-calculated tabulation. The resulting wall/fluid heat transfer rate (along with the other terms for heat flows in FEM simulations) is used to model the temporal evolution of the temperature in the solid, including the influence of cooling fluid.

Figure 3 shows an example of a detailed field at a boundary layer fluid flow (iso-octane/air, initially at 350 K) along a wall with temperature of 700 K. The wall-normal temperature gradient at the fluid/wall interface is of paramount importance for the heat transfer; for fully resolving this gradient, a spatial resolution of better than 50 μm is typically required. Note how the gradient decays from left to right, by the increasing contact time between fluid and wall in downstream direction.

Figure 3 b) is an excerpt from the tabulation of the temporal development of the effective heat transfer rate coefficient α in a boundary layer flow (99% air, 1% iso-octane) along a wall with 850 K surface temperature, as a function of overall mass flow rate. A very weak dependence of α on mass flow rate is found, while the fluid/wall contact time is a major influence.

These pre-calculated heat transfer coefficients allow combining the full resolution and detail of the heat transfer simulations in simple geometries with the complex geometries of realistic machining processes at low computational cost. In particular, the extremely large computational effort for fully resolving the near-wall temperature gradients in the fluid as well as computing the complex state dependence of the fluid properties can be decoupled from the actual FEM simulation.

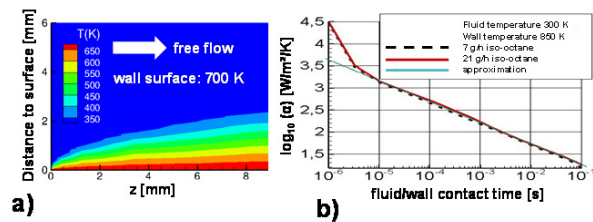


Figure 3: a) Temperature field in a boundary layer fluid flow and b) Tabulation of the temporal development of the effective heat transfer rate coefficient

2.3. Development of the 2D simulation

In earlier works [16], a 2D finite element model of the orthogonal cutting process has been introduced to calculate and analyse changes in the microstructure such as the phase transformations for dry machining. This model allows the prediction of phase transformations, temperatures and forces.

The substructure of the model depicts a coupled thermo-mechanical material behaviour with a user defined material model. The fixed workpiece and a moving tool are combined in the Lagrangian modelling approach. Furthermore, a remeshing routine is implemented in the model.

The temperature field with regard to the friction, plastic deformation and even latent heat of the phase transformation and its enthalpy is considered as an input parameter to simulate the phase transformations.

The latest developments of this model are the additions mentioned in this paper. In terms of the development of the friction coefficients, the existing friction model has been updated. This model assigns the friction coefficients to the contact area workpiece and tool depending on the temperature and relative velocity. These parameters have been changed with the experimental MQL results.

The information calculated in the fluid flow simulation part is yet limited to the flank face. Therefore, it has to be considered that equation (1) describing the influence of the MQL is only used in the range of validity of the model.

$$\log_{10}(\alpha) = a - b * \log_{10}(t) \quad (1)$$

with the regression parameters $a = 6.2$ and $b = -0.47$.

To ensure that the defined MQL load only affects the flank face of the workpiece, the user subroutine film is used in Abaqus to describe the changed heat flow and heat transfer coefficients, see Figure 4.

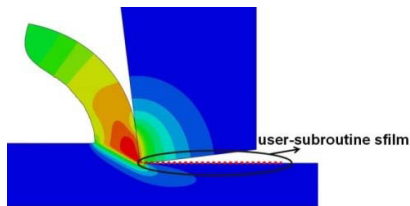


Figure 4: Range of validity for the user-subroutine sfilm

2.4. Development of the 3D drilling simulation

The developed 3D model with its boundary conditions and materials laws according to [17] represents the kinematics of the drilling process for the workpiece in Figure 5 a). Just as the 2D simulation model, this drilling model also comprises of a submodel which calculates the phase transformation during the diffusive and non-diffusive transformation process. The diffusive transformation description is based on a modified approach by Avrami and the non-diffusive one by Skrotzki according to Koistinen & Marburger.

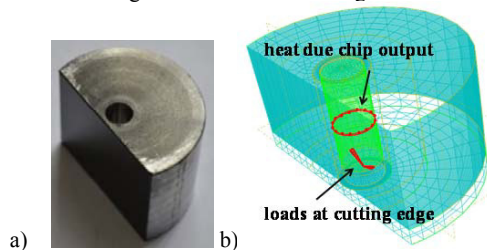


Figure 5: a) Used workpiece for the experiments, b) simulation model with different thermal and mechanical loads

The thermal and mechanical load for the kinematics of the drilling process is divided into 2 mechanisms. The first one consists of the thermal and mechanical load at the cutting edge of the drilling tool. The loads are penetrating one plane further into the model with every full rotation of the tool taking into account the feed rate of the drilling process. Therefore, the forces and temperatures are calculated in the 2D simulation and are implemented directly as an element set for the forces and node set for the temperatures into the 3D model along the cutting edge of the used drilling tool. These results are compared with experimental tests to validate the simulation findings. An orthogonal turning process has been chosen for the experimental measurements. While the cutting velocity varies along the cutting edge of the drilling tool, different specific spots on the cutting edge are selected and compared to the turning results with the same cutting speed. The applicability of this method has already been proven and is explained in detail in [17]. The advantage of this procedure lies in the ability to validate the 2D model with only one experimental test, requiring merely one simple measurement strategy.

The second load mechanism takes the hot drilling tool and the chips into account. The temperatures of the workpiece are measured at different positions in feed direction of the drilling hole in order to model this thermal effect, as illustrated in Figure 7. Experiments need to be performed to obtain these temperatures because 2D simulations do not reveal this information.

In contrast to the 2D model, the 3D drilling model does not require new friction or heat transfer models since the temperature and the forces are implemented directly into the model due to the element and node sets.

2.5. Experimental set-up for the 3D drilling simulation

The experiments are performed on the machining centre Heller MC16 for drilling tempered steel AISI 4140. The equipment to measure the temperatures and forces consist of a Pyrometer “FIRE-II” for the temperature propagation and a Kistler multicomponent dynamometer type 9215A for the forces mounted on the tool holder. The experiments extend the experimental work of [17] to ensure the comparability of the results.

First of all, the workpiece illustrated in Figure 5a) needs to be prepared for the temperature measurements. Four holes are drilled into the circular side of the workpiece using micro electro discharge machining (μ EDM). It has been ensured that the μ EDM-holes end close to the surface of the drilling hole, meaning that no passage is created. The four holes (see Table 2) are lined orthogonally in feed direction of the drilling hole (Figure 7). So the temperature of the surface wall is measured and not the temperature of the MQL. This measure allows to capture the temperature development at the surface of the drilling hole time dependent in various stages of the process. The dimension of the workpiece is presented in Figure 6.

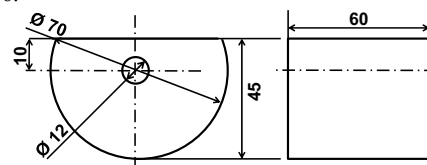


Figure 6: Dimension of the workpiece

The drilling experiments were performed with Walter ALPHA4 drilling tools. These tools have a diameter d of 12 mm, a overall length of $5x d$, a nose angle of 140° and a TiAlN multilayer coating with two MQL channels.

Table 2 Measuring positions

Position of the pyrometer fibre	1	2	3	4
Distance from top of the workpiece [mm]	6	12	18	24

In the next step, the temperatures and forces are measured during turning. Therefore, a cylindrical workpiece with constant webs is turned five times at every cutting speed, see Figure 8 to the right. The cutting speed is adapted to selected basis points on the cutting edge of the drilling tool. These

basis points consist for example of the outer end of the cutting edge or the middle point of the cutting edge. Every basis point has a different cutting speed and in turn is used for the associated turning experiment.

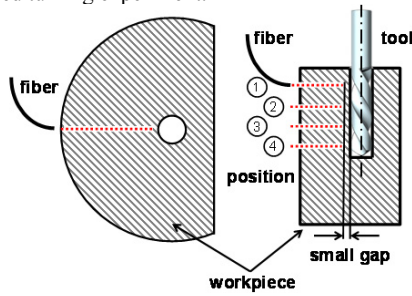


Figure 7: Measuring position for the pyrometer in the workpiece

The temperature is measured once more with the pyrometer “FIRE-II” and the forces with the Kistler multicomponent dynamometer type 9215A. For cutting tool a μ EDM drilled insert is chosen, see Figure 8 to the left.

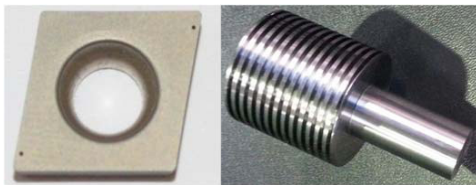


Figure 8: Cutting tool and workpiece

3. Results

3.1. 2D FEM simulation

The results of the 2D models have been evaluated at a cutting distance of 1 mm. This distance ensures a thermal equilibrium in the cutting process to impede the calculated maximum temperatures from altering significantly at any following position.

The maximum temperatures for dry and MQL cutting are presented in Figure 9 and Figure 10. It can be seen that the temperatures in dry and MQL cutting raise when higher cutting speeds are performed. The effect of MQL results in a constantly lower temperature level of about 175°C compared to dry cutting. This difference in temperature has also been noticed in the friction experiments where the temperature has been measured as well. The presumption that MQL substantially reduces the temperature development through lower friction coefficients has been affirmed. In addition, the maximum temperature at the highest cutting speed is almost as high as the maximum temperature at the lowest cutting speed in dry cutting. This is a first affirmation of the high potential of MQL machining. The higher temperatures in dry cutting lead to a higher thermal load in the workpiece. When a critical temperature is reached, austenite and martensite transformation start at the surface.

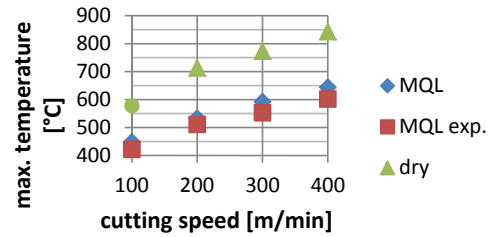


Figure 9: Temperature developments for different cooling methods during simulation and in experiments

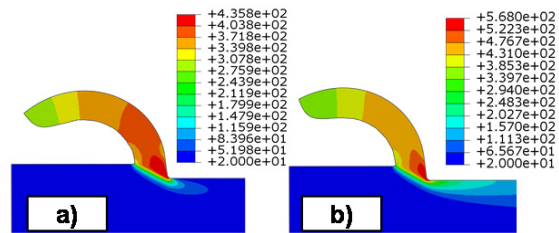


Figure 10: a) Temperature [°C] developments for MQL and b) dry cutting

During simulation, a martensitic change in the microstructure is defined as a martensitic phase transformation of more than 1 volume percentage. The results for dry cutting show that first parts of the microstructure are transformed to martensite at a cutting speed of 200 m/min, see Figure 11. A full transformation is almost completed at 300 m/min. There are no changes in the microstructure during all cutting speeds calculated due to the lower maximum temperatures for the simulation with MQL.

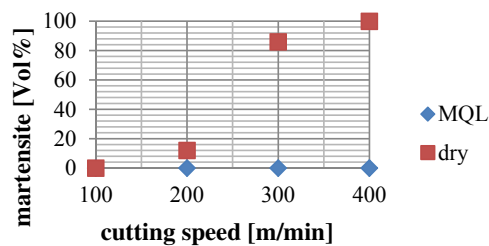


Figure 11: Phase transformations for dry and MQL cutting

A look at the cutting forces reveals a lower behaviour for the MQL process, see Figure 12. The decrease of the cutting forces in dry machining is higher than the decrease with MQL. At high cutting speeds, the positive effect of MQL declines. Although, dry cutting and MQL cutting nearly feature the same cutting force at a cutting speed of 400 m/min. The experimental results show a better agreement for higher cutting speeds than for lower speeds. However, the percentual deviation from experiment to MQL simulation amounts to less than 10%.

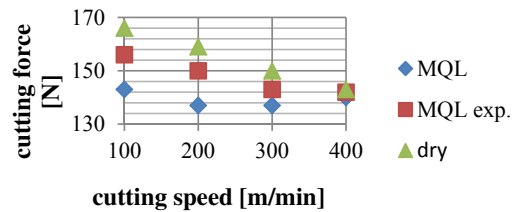


Figure 12: Comparison of the cutting forces

3.2. 3D FEM simulation

With the developed 3D drilling model, a number of simulations have been performed to obtain a deeper insight into the cutting process with MQL. The main aim of the model is to predict temperatures and phase transformations during the cutting process of the material. Figure 13 shows on the left side the temperature distribution for the dry cutting and the MQL process on the right. It can be seen, that the maximum temperatures in the MQL simulation are essentially lower than in dry cutting. Due to the use of MQL, the extremely hot areas at the end of the cutting edge decrease and a more homogenous temperature distribution arises. This can be explained by the use of MQL, which reduces the hot local temperatures.

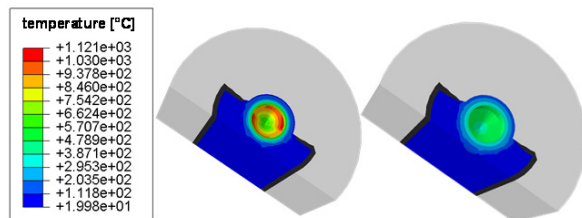


Figure 13: Temperature distribution for dry drilling (left) and MQL (right)

In addition to the temperature and the temperature distribution, the drilling induced phase transformations on the surface of the drilling hole have been calculated. Special regard has been paid to the martensitic transformation at the surface. Like the results in the 2D simulation, there are also no microstructural changes for the 3D drilling simulation with MQL. The comparison to the dry 3D drilling simulation shows that higher maximum temperatures lead to a martensitic surface layer. It has to be noted that the martensitic equal scatter in the model is of too large segmentation in this area. Further simulations have to be performed with a finer segmentation. This step should rectify this problem and a more detailed solution of the phase transformation will enhance the resolution.

4. Summary and Conclusion

This paper presents simulations of a MQL machining process. The precomputed, parameter-dependent effective heat transfer coefficients taken from detailed, fully resolved 1D fluid flow computations are used in the FEM simulations. The FEM simulations agree well with experimental results. The consideration of MQL in FEM simulations of

temperature, forces and phase transformations during machining operations allows to predict differences between MQL and dry processing. This can be seen in the changes of the microstructure such as surface hardening. The improved description of the heat transfer process also aids the process understanding by FEM simulations.

Acknowledgements

The authors gratefully thank the Deutsche Forschungsgemeinschaft DFG for the support of the priority program 1480 "Modelling, Simulation and Compensation of Thermal Effects for Complex Machining Processes".

References

- [1] Bhowmick S, Alpas AT. The role of diamond-like carbon coated drills on minimum quantity lubrication drilling of magnesium alloys. *Surface & Coatings Technology* 205 (2011). pp. 5302-5311.
- [2] Attanasio A, Gelfi M, Giardini C, Remino C. Minimal quantity lubrication in turning: Effect on tool wear. *Wear* 260 (2006). pp. 333-338.
- [3] Rahman M, Senthil Kumar A, Salam MU. Experimental evaluation on the effect of minimal quantities of lubricant in milling. *International Journal of Machine Tools & Manufacture* 42 (2002). pp. 539-547.
- [4] Braga DU, Diniz AE, Miranda GWA, Coppini NL. Using a minimum quantity of lubricant (MQL) and a diamond coated tool in the drilling of aluminum-silicon alloys. *Journal of Materials Processing Technology* 122 (2002). pp. 127-138.
- [5] Hadad M, Sadeghi B. Minimum quantity lubrication-MQL turning of AISI 4140 steel alloy. *J. of Cleaner Production* 54 (2013). pp. 332-343.
- [6] Stephenson D.A., Skerlos S.J., King A.S., Superkar S.D. Rough turning Inconel 750 with supercritical CO₂-based minimum quantity lubrication. *J. of Materials Processing Technology* 213 Issue 3 (2014). pp. 673-680.
- [7] Tasdelen B, Wikblom T, Ekered S. Studies on minimum quantity lubrication (MQL) and air cooling at drilling. *Journal of Materials Processing Technology* 200 (2008). pp. 339-346.
- [8] Aurich JC, Fallenstein F. CFD-Simulation der Kühlung von innengekühlten VHM-Wendelbohrern. *VDI-Z* 2 (2013). pp. 48-51.
- [9] Chen M, Jian L, Shi B, Liu Z, An Q. CFD Analysis on the Flow Field of Minimum Quantity Lubrication during External Thread Turning. *Materials Science Forum* Vol. 723 (2012). pp. 113-118.
- [10] Obikawa T, Asano Y, Kamata Y. Computer fluid dynamics analysis for efficient spray of oil mist in finish-turning on Inconel 718. *International Journal of Machine Tools and Manufacture* 49 (2009). pp. 917-978.
- [11] López de Lacalle LN, Angulo C, Lamikiz A, Sánchez JA. Experimental and numerical investigation of the effect of spray cutting fluids in high speed milling. *J. of Materials Processing Tech.* 172 (2006). pp. 11-15.
- [12] Pervaiz S, Deiab I, Wahba EM, Rashid A, Nicolescu M. A coupled FE and CFD approach to predict the cutting tool temperature profile in machining. *Procedia CIRP* 17 (2014). p. 750-754.
- [13] Shu S, Cheng K, Ding H, Chen S. An Innovative Method to Measure the Cutting Temperature in Process by Using an Internally Cooled Smart Cutting Tool. *J. of Manufacturing Science and Eng.* 135 (2013). 061018.
- [14] Schumann S, Metzger M, Hartmann H, Biermann D. Simulativer Vergleich unterschiedlicher Kühlkonzepte beim Bohren - FE-gestützte Darstellung der thermischen Bauteilbelastungen bei der Trocken- und Nassbearbeitung sowie der CO₂-Schneestrahlkühlung beim Bohren. *wt Werkstattstechnik online Jahrgang 104 (2014) H. 1/2*. pp. 16-21.
- [15] Schulze V, Michna J, Zanger F, Pabst R. Modeling the process-induced modifications of the microstructure of work piece surface zones in cutting processes. *Adv. Materials Research* Vol 223 (2011). pp 371-380.
- [16] Maas, U. Detailed Numerical Simulation of Chemically Reacting Flows. In *Detailed Numerical Simulation of Chemically Reacting Flows*, Proc. International Symposium on Computational Fluid Dynamics (1991), p. 741.
- [17] Schulze V, Zanger F, Michna J, Lang F. 3D-FE-Modelling of the Drilling Process - Prediction of Phase Transformations at the Surface Layer. 14th CIRP Conference on Modeling of Machining Operations.